Color Enhancement of Highly Correlated Images. I. Decorrelation and HSI Contrast Stretches

ALAN R. GILLESPIE,* ANNE B. KAHLE, AND RICHARD E. WALKER

Jet Propulsion Laboratory, California Institute of Technology, Pasadena, California 91109

Conventional enhancements for the color display of multispectral images are based on independent contrast modifications or "stretches" of three input images. This approach is not effective if the image channels are highly correlated or if the image histograms are strongly bimodal or more complex. Any of several procedures that tend to "stretch" color saturation while leaving hue unchanged may better utilize the full range of colors for the display of image information. Two conceptually different enhancements are discussed: the "decorrelation stretch," based on principal-component (PC) analysis, and the "stretch" of "hue"–"saturation"–intensity (HSI) transformed data. The PC transformation is scene-dependent, but the HSI transformation is invariant. Examples of images enhanced by conventional linear stretches, decorrelation stretch, and by stretches of HSI transformed data are compared. Schematic variation diagrams or two- and three-dimensional histograms are used to illustrate the "decorrelation stretch" method and the effect of the different enhancements.

Introduction

Multispectral images used in remote sensing are generally prepared for interpretation by selecting three of the image channels for display as red, green, and blue (R, G, and B) components of an additive color picture. Spectral information contained in the data is portrayed in the colors of the displayed picture. It is advantageous to create colorful pictures in order to convey as much spectral information as possible to the photointerpreter. In many images, this goal is easily achieved because the spectral data are not highly correlated from channel to channel, and thus the displayed pictures contain a wide range of colors. Multispectral images of spectrally featureless scenes are highly correlated from one channel to the next, however, and color pictures made from such images are generally monochromatic. The spectral information that is in the scenes is not easily extracted from the displayed picture; yet this information may be critical to the analyst.

Contrast exaggeration or "stretching" of the three highly correlated image channels displayed as R, G, and B serves mainly to expand the dark–light range of intensities; it does little to expand the range of colors displayed, and a picture of the stretched image still appears monochromatic. In order to display highly correlated images as colorful pictures, it is necessary to exaggerate the least correlated part of the information selectively; i.e., to decrease the correlation. Essentially, this corresponds to exaggerating the color saturation (chroma or purity), independent of the lightness. It is generally desirable to leave the distribution of hues alone. There are several techniques for achieving these goals. In this article, two of these techniques are explored: (1)

*On assignment to the Department of Geological Sciences, University of Washington, Seattle, WA 98195.

0034-4257/86/$0.00

stretching of "decorrelated" images and (2) stretching of "hue"–"saturation"–saturation"–intensity (HSI) transformed images.

Data describing a scene (object domain) are acquired as images (image domain) and displayed as pictures (display domain), ultimately to be perceived by the photointerpreter. In each domain there is different nomenclature to describe the stimulus ultimately perceived as color. Radiant fluxes from the object domain are measured and integrated over time and a range of wavelengths and converted to numbers (DN, or "data numbers") in the image domain. DN from the scanners discussed in this article vary linearly with the radiant fluxes they describe. They are thus measures of energy, or intensity.

In order to be viewed, images must be displayed. To do this, the image intensities are converted to electrical impulses that are used to control beam intensities in a cathode ray tube, or in one of several kinds of devices that create pictures on paper or photographic films. Only if the transfer functions that relate radiant fluxes from the displayed picture to image DN are the inverses of the functions that relate the image and object domains will the displayed picture faithfully describe the object domain. This is not necessarily the case—most CRTs, for example, emit light proportional to $DN^{-\gamma}$, where γ is some characteristic constant (e.g., Foley and Van Dam, 1982). Considerable effort has been invested in understanding display devices and in compensating data both in the image domain and during playback so that the displayed picture is a linear representation of the object domain. The reader is referred to Meyer and Greenberg (1980), Catmull (1979), and Smith (1978) for discussions of this subject.

Color pictures are created by assigning primary colors red (R), green (G), and blue (B) to three planes or channels of image data, taken in different spectral bands. Many images are acquired at wavelengths outside the visible spectrum; thus pictures displaying these data are often called "false" color.

In the display domain color information is described by a number of "psychophysical" parameters (Wyszecki and Stiles, 1967). Tristimulus values are the amounts of the three primary colors, R, G, and B, required to produce a given color. Chromaticity coordinates are the ratios of each tristimulus value of the color to their sum.

Colors in the display domain are perceived by the photointerpreter. Perceived colors have three attributes: hue, saturation, and lightness. It is common practice to describe colors in the display domain by their perceived attributes, and it is becoming common to even "project" these descriptions back to the image domain. A DN or intensity triplet may be described in terms of the perceived color it produces. This confusing practice is useful in that it facilitates intuitive understanding and manipulation of data in the image domain. In this article, where we adhere to this practice we enclose the name of the perceptual attribute in quotation marks.

The manipulations we describe in this article are applied in the image domain. We regard the display domain as an imperfect representation of the image domain, but one that can be made to have a close correspondence. Color pictures used in this article were created by sequential exposure of color negative film to the

chosen image channels through *R*, *G*, and *B* filters in JPL's GRE and Dicomed playback devices. The transfer functions relating image intensities and light transmitted through the negative film for the GRE were linear. The Dicomed function is exponential. The effect of exponential playback is to shift colors towards saturated and primary hues (Appendix A).

"Decorrelation stretching" was introduced by Soha and Schwartz (1978), augmenting earlier work by Taylor (1973). The technique is based on a principal-component (PC) transformation of the acquired data. Often, such transformed images themselves are contrast-stretched and arbitrarily assigned primary colors for display as a color composite picture. "Decorrelation stretching" differs in that after contrast enhancement the statistically independent (decorrelated) PC images are retransformed to the original coordinates for display, so that in general there is little distortion of the perceived hues due to the enhancement. This makes interpretation of the enhanced images reasonably straightforward. Stretching of the decorrelated images serves mainly to exaggerate color saturation. Several examples of the effective use of the decorrelation stretch have been published in the last few years (Kahle et al., 1980; Kahle and Rowan, 1980; Kahle and Goetz, 1983; Gillespie et al., 1984; Abrams, 1984).

The *HSI* transformation is a standard technique for numerically describing color in the image domain, using spherical coordinates roughly analogous to the conventional perceptual attributes hue (*H*), saturation (*S*), and lightness (*I*) (Gillespie, 1975; Soha et al., 1976; Raines, 1977; Ruiz et al., 1977; Gillespie, 1980). We refer to the *HSI* parameters as "hue," "saturation" and intensity (the last is valid image-domain terminology.) Although *HSI* and Munsell coordinates (Wyszecki and Stiles, 1967) roughly correspond, the two systems are not affine and the *HSI* values should not be regarded as Munsell coordinates. *HSI* coordinates map the image domain. Munsell coordinates describe colors in the object and/or display domain.

Unlike the PC transformation, the *HSI* transformation is scene-independent or invariant. Stretching the *S* and *I* images independently is a simple and understandable way of creating effective color pictures that retain approximately the original distribution of hues (Gillespie, 1980; Haydn, 1981; Haydn and Youssef, 1984; Kruse and Raines, 1984). As in the decorrelation stretch method, the images are retransformed to the original *RGB* coordinate system for display. Although the *HSI* transformation was designed for color analysis and enhancement, it has also been used to combine three different registered data sets for display as color pictures (e.g., Haydn, 1981; Daily, 1983).

A major strength of the enhancement methods presented in this article is the ease with which the processed pictures can be related by the photointerpreter to the images as acquired. This greatly facilitates understanding the displayed image data in terms of spectral properties of the imaged surface. Many other approaches that yield dramatic and colorful pictures of highly correlated images of spectrally flat scenes (e.g., Berlin et al., 1976; Fig. 31-176 and 31-202 in Williams, 1983; Thomas and Nicholas, 1984) do not share this interpretive simplicity.

With the availability now of very highly correlated multispectral data, such as from the NASA Thermal Infrared Multispec-

tral Scanner (TIMS) (Palluconi and Meeks, 1985), we find that it is appropriate to discuss details of image color enhancement techniques, along with their potential advantages and limitations. In this article we first describe conventional color enhancement by independent contrast adjustment of individual image channels. We then introduce the decorrelation and *HSI* enhancements, and compare pictures of the same images enhanced by the different methods. We use schematic diagrams to illustrate steps in the enhancement processes, and to compare the results shown by the image examples. Finally, we illustrate some ways in which the enhancements may yield undesired results. It is our hope that this discussion will promote more widespread and effective use of appropriate color enhancement techniques for the display of highly correlated image data. A second article describing different enhancement techniques, based on channel ratioing, is forthcoming (Gillespie et al., 1986).

Conventional Contrast Stretching of Poorly Correlated and Highly Correlated Data

Conventional contrast stretching of the individual channels to be displayed in red (R), green (G), and blue (B) has proven to be an effective method of enhancement for color composite pictures of many images taken in the visible and reflected infrared regions of the spectrum (e.g., Landsat MSS data.) This is because the scenes already contain a wide range of strongly colored objects (poorly and moderately correlated data) in these wavelengths [Table 1(a)]. Conventional linear contrast stretching is illustrated schematically in Fig. 1 for two channels of image data. Figure 1 shows variation diagrams or two-dimensional histograms in which the axes are the intensities for the two channels A and B and in which the contoured variable is the number of times a given pair of intensities is encountered in the image. The two channels of data are taken to have similar variances. (For n channels of data, similar variation diagrams can be constructed in n-space.)

In poorly correlated data [Fig. 1(a)] many different DN pairs are encountered away from the equal-intensity ("achromatic") line $A = B$, and the contours form roughly equidimensional outlines. Contrast adjustment serves to expand (or contract) the DN cluster parallel to the axes or, as shown, to change the scale of the axes and to translate (but not to rotate) them with respect to the cluster. This increases the number of different DN pairs enclosed by the cluster. In three dimensions, the effect is to increase the diversity of colors in the picture. The stretch is chosen to fill the entire intensity range for each channel, without saturating too much data on either end of that range.

For highly correlated data [Fig. 1(b)] the cluster is highly elongate. Fewer DN pairs are encountered away from the line $A = B$ than for poorly correlated data. Stretching the A and B axes to A' and B', using the same criteria as for Fig. 1(a) does not significantly decrease the oblateness of the cluster, and, although the black–white range may be more effectively utilized, it is unlikely that the range of colors displayed would be satisfactory to the photointerpreter.

Most available DN pairs in Fig. 1(b) lie outside the cluster, and are unoccupied. More severe contrast increase (A'' and

TABLE 1 Correlation Matrices for (a) Typical Landsat MSS Data, (b) the Unusual Bimodal MSS Data of Fig. 3, and (c) the TIMS data of Fig. 4[a]

(a)	MSS	4	5	7	
	4	1.00			Cape Mendocino,
	5	0.92	1.00		Humboldt County,
	7	0.59	0.52	1.00	CA
(b)	MSS	4	5	7	
	4	1.00			Pisgah Crater,
	5	0.98	1.00		Mojave Desert,
	7	0.94	0.98	1.00	CA
(c)	TIMS	1	3	5	
	1	1.00			Trail Canyon,
	3	0.98	1.00		Death Valley,
	5	0.92	0.87	1.00	CA

[a] Image channel numbers are shown above and left of the matrices.

B'' axes) does decrease the oblateness of the cluster and fill most of the DN pairs, but this is achieved only by saturating most of the data in the image, or by forcing the range of the data to exceed the black–white range of the display device. Thus conventional contrast stretching of individual channels of highly correlated data is not an effective method of color enhancement.

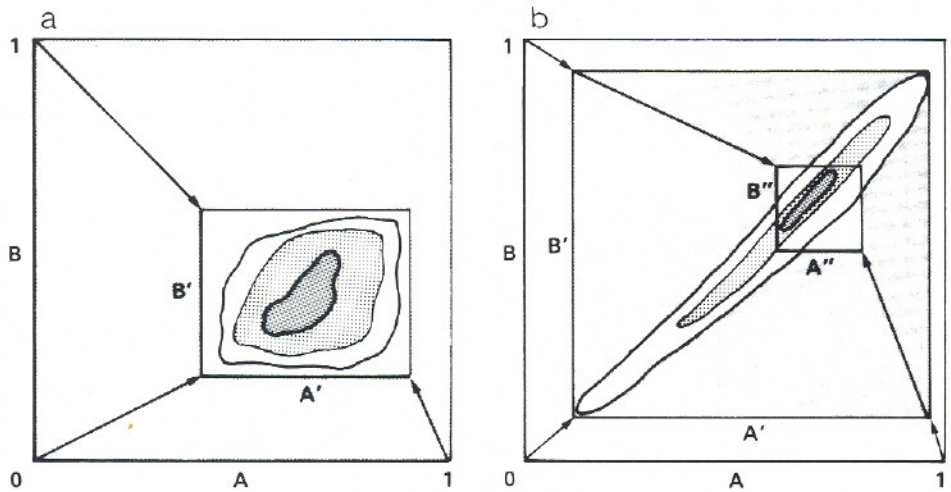

FIGURE 1. Schematic variation diagrams showing the effects of linear stretches for two channels A and B of (a) poorly correlated and (b) highly correlated data. Variances for the two channels of data are similar. Contour lines describe the probability density for intensity pairs (A, B). Outer axes show scaled intensities ranging from 0 (black) to 1 (white). The acquired data do not fill the entire dynamic range; contrast "stretching" adjusts the range so that they do (inner axes). Correctly displayed in a color picture, data on the line $A = B$ will be gray; other data will be colored. For Fig. 1(a), stretching A and B independently results in the contoured cluster filling the (A', B') plane, or in a wider range of colors in the enhanced picture. For Fig. 1(b), stretching to the A' and B' axes leaves most intensity pairs unoccupied. The enhanced picture is mainly gray. More extreme stretching to A'' and B'' results in a wider range of colors, but most data fall outside the dynamic range and much chromatic information is lost.

The Decorrelation Stretch

Method

The decorrelation stretch involves expanding the DN cluster of highly correlated data shown in Fig. 1(b) along its principal axes instead of along the A and B axes. These principal axes (P_1, P_2) are shown in Fig. 2(a). They are statistically independent in that the covariance of the calculated P_1 and P_2 data values is zero. The principal axes are numbered in order

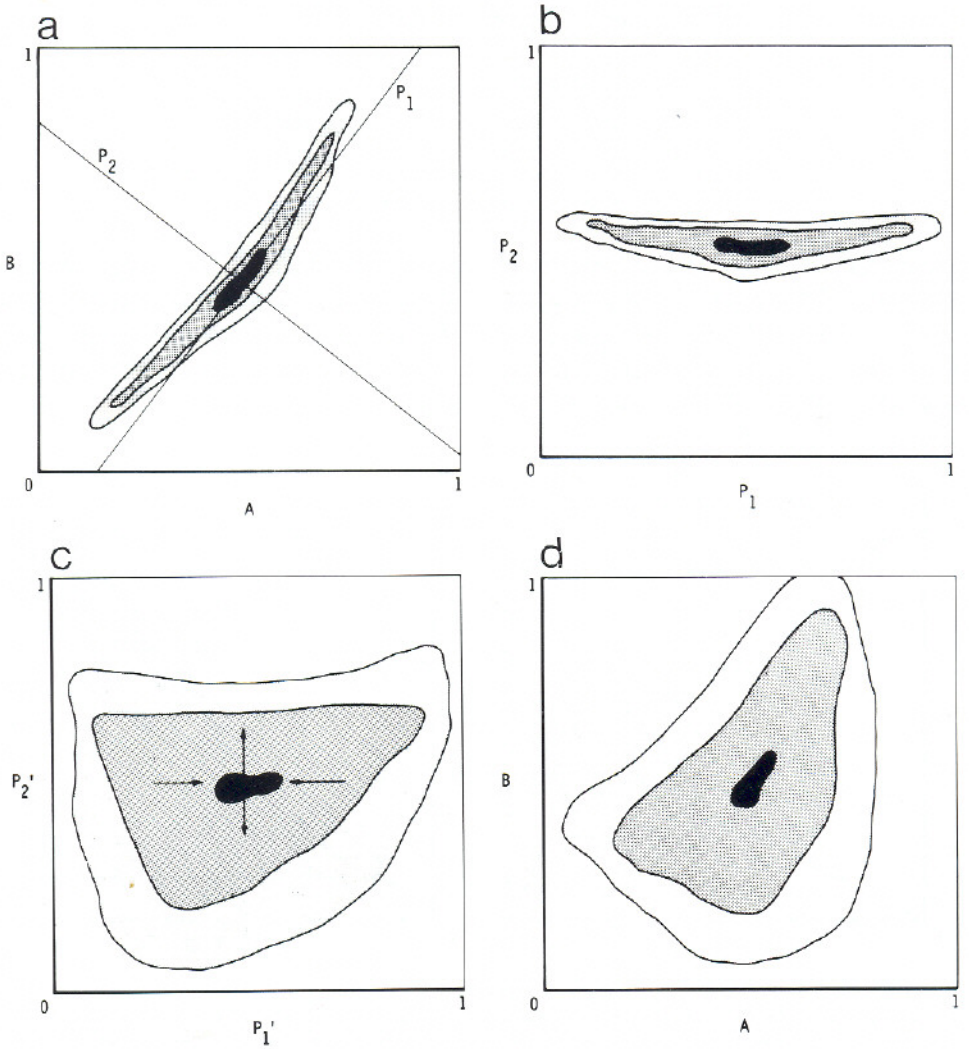

FIGURE 2. Schematic representation of decorrelation stretching for highly correlated data. (a) Variation diagram of data (A, B) as acquired, showing the orthogonal principal axes P_1 and P_2. (b) Data cluster after principal-component transformation, followed by an arbitrary translation such that there are only nonnegative values. (c) Linear contrast stretches applied to the "decorrelated" P_1 and P_2 channels. The stretches are chosen to equalize the variances in P_1 and P_2. Arrows show the relative sense of the expansion of the data cluster to fill the data plane (P_1 is stretched much less than P_2, or even compressed). (d) The stretched data returned to the (A, B) coordinate system by the inverse transformation. The cluster now fills the plane and the data are displayed with a wide range of colors.

of descending variance (or eigenvalues), so that P_1 describes the major lightness fluctuations in a scene (e.g., albedo and topographic shading), while P_2 describes deviations from P_1, or from the average color of the scene. Selectively increasing the contrast along P_2 thus will tend to exaggerate image color. The decorrelation stretch is performed after transforming the acquired data to the (P_1, P_2) coordinate system.

Geometrically, this principal-component transformation involves rotation and translation of the A and B axes [Fig. 2(b)]. The PC transformation itself has been widely published (e.g., Pearson, 1901; Hotelling, 1933; Gonzales and Wintz, 1977) and is not repeated here. The origin of the (P_1, P_2) axes coincides with the centroid of the data cluster, but usually the axes are translated so that the entire cluster lies within the first quadrant (nonnegative values). The P_1 and P_2 images are then stretched independently, as shown in Fig. 2(c). Usually the stretches are linear expansions chosen to equalize the variance, although Soha and Schwartz (1978) instead used nonlinear stretches that caused the data distribution to become Gaussian. Either way, the stretches expand the cluster to fill much or most of the data plane. Finally, the inverse of the PC transformation (including the translation to the first quadrant) is applied, so that the A and B axes are recovered [Fig. 2(d)]. These data, now poorly correlated, are then displayed (in the three-dimensional case) as a color composite picture.

Because it is based on PC analysis, decorrelation stretching is readily extended to any number of image channels. In this respect it differs from the *HSI* technique, which is applied to only three channels. The generality of PC analysis is useful if color pictures of different triplets of channels from the same image are to be compared.

Decorrelation stretch of a Landsat MSS image

In Fig. 3 we present color composite pictures of three of the four channels of a Landsat MSS image of Pisgah Crater, in the Mojave Desert of California, before and after color enhancement by the decorrelation–stretch method. The scene contains materials with a wide range of albedos: dark basalt flows and bedrock outcrops darkened by desert varnish, and lighter alluvial fans, windblown sand, and playa deposits. Figure 3(a) was produced in the conventional manner, by linear contrast stretching of each channel independently. Because the DN distributions (histograms) for each channel are strongly bimodal (light alluvium and dark lava), data from the three image channels are more highly correlated than is usual for Landsat images [Table 1(b)]. Linear stretches are not able to expand the two modes of DN to make adequate use of the available colors in the displayed picture. Figure 3(b) was produced by decorrelation stretching. In this picture the range of lightness is reduced, and the range of chromaticness (hue and saturation) is expanded compared to Fig. 3(a). More effective use is made of the color display. Decorrelation stretching may reduce between-channel correlation coefficients for MSS data from the high values of Table 1(b) (> 0.9) to values of 0.3 or less (M. Podwysocki, personal communication, 1986.)

Decorrelation stretch of a multispectral thermal infrared image

In Fig. 4 we present color composite pictures made from three channels of a

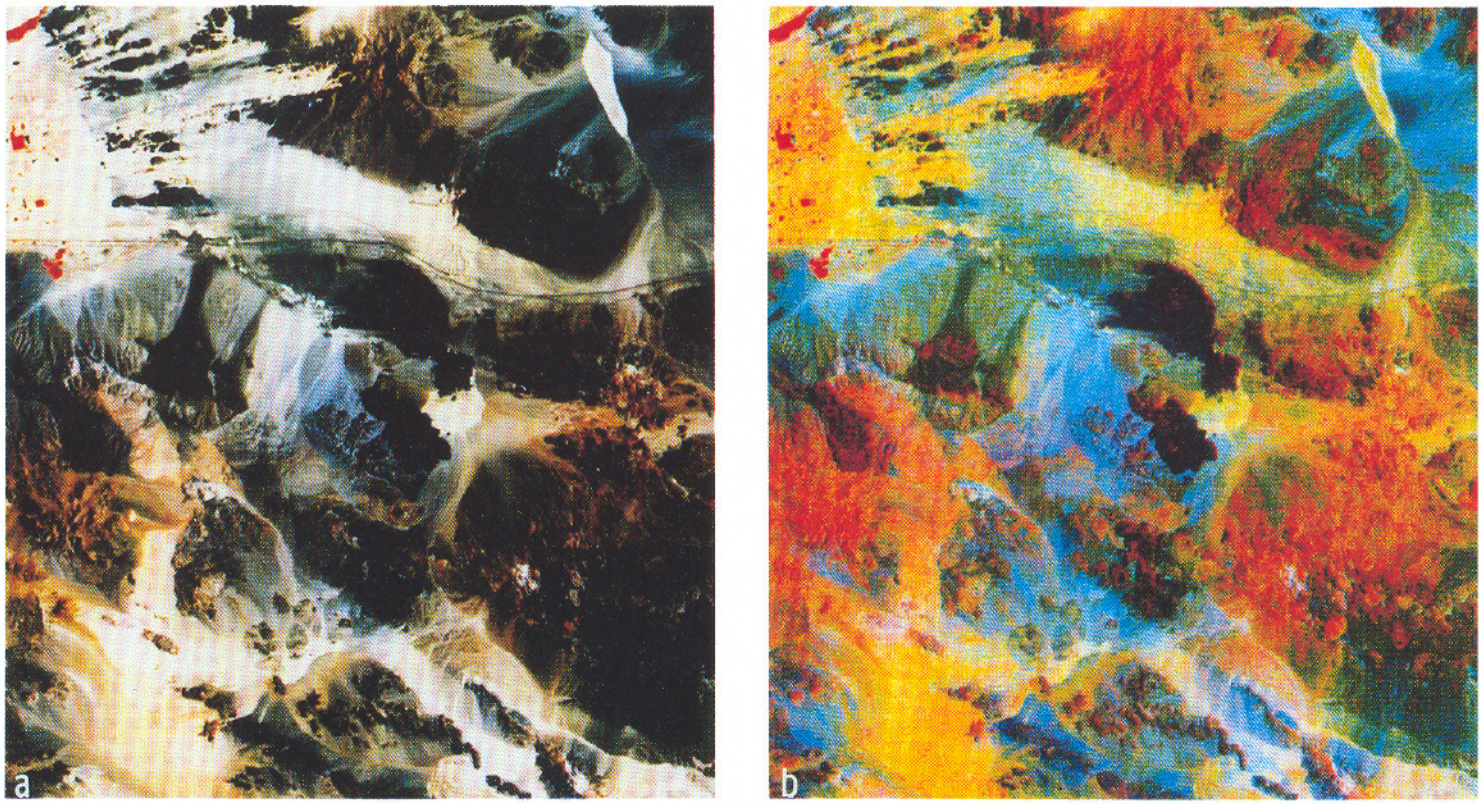

FIGURE 3. Part of JPL's digital mosaic of Landsat MSS images of California, centered on Pisgah Crater in the Mojave Desert: (a) linear stretch on each channel independently; (b) decorrelation stretch. Color pictures were made from MSS channels 4 (0.5–0.6 μm), 5 (0.6–0.7 μm), and 7 (0.8–1.1 μm) assigned to B, G, and R, respectively (GRE playback).

multispectral thermal infrared TIMS image of Trail Canyon fan in Death Valley, California (Kahle and Goetz, 1983; Gillespie et al., 1984) before and after color enhancement by the decorrelation–stretch method. A target showing colors for selected realistic temperature and emittance values has been affixed to each version. The target was processed identically to the image, so that values of these parameters in the image may be estimated from inspection of the target. The data as acquired are shown in Fig. 4(a); the data after conventional linear stretches of each channel independently are shown in Fig. 4(d).

Emitted thermal infrared radiation is the product of blackbody radiation and the emittance of the radiating surface. The emittance varies with wavelength and is different for different surface materials. In principle, emittances may range from 0 to 1, but for most natural surfaces they vary over only a small fraction of that range, bracketed by the values in the color targets (Kahle and Walker, 1984). Thus the measured thermal radiance is dominated by the blackbody component, which depends on the temperature. For the limited temperature ranges of less than (for example) 30°C commonly encountered in terrestrial scenes, the blackbody curves have similar shapes, so that the radiance data are highly correlated among channels. This is shown by the correlation matrix for the multispectral image of Fig. 4 [Table 1(c)]. The extent to which the thermal radiance data are *not* correlated is due mainly to the presence in the scene of materials having structured emittance spectra.

Conventional contrast stretching of the individual channels displayed as R, G, and B [Figs. 4(b) and 4(c)] serves mainly to adjust the lightness rather than to expand the chromaticness of the color composite picture, because the dominant temperature information varies little from channel to channel. The limited range of colors after a moderate stretch is apparent in Fig. 4(b). More severe contrast stretches applied to the individual channels saturate large amounts of data on either end of the black–white intensity scale without substantially increasing the amount of perceived color [Fig. 4(c)].

The decorrelation stretch, however, increases the range of colors in the displayed picture [Fig. 4(d)]. Comparison with Figs. 4(b) and 4(c) shows that hues are reasonably well preserved in this operation. Decorrelation stretches obviously tend to increase saturation as well as modifying the range of lightness while affecting the hues little. This is useful in displaying the poorly correlated data for interpretation. In Fig. 4(d) it is the poorly correlated emittance component of the data that is exaggerated, rather than the highly correlated temperature-dependent component. Thus by using the decorrelation stretch, information about the composition, rather than the temperature alone, is made available to the photointerpreter.

Variation diagrams for decorrelation-stretched images

Highly correlated and decorrelated clusters of image-domain data are shown in three dimensions (RGB) in Figs. 5(a) and (b). Projection of the data clusters from Fig. 5 onto the plane $B + G + R = 1$ [Figs. 6(a) and (b), respectively] gives a ternary variation diagram analogous to the conventional tristimulus chromaticity diagram (e.g., Wyszecki and Stiles, 1967). Image-domain "chromaticity" values r',

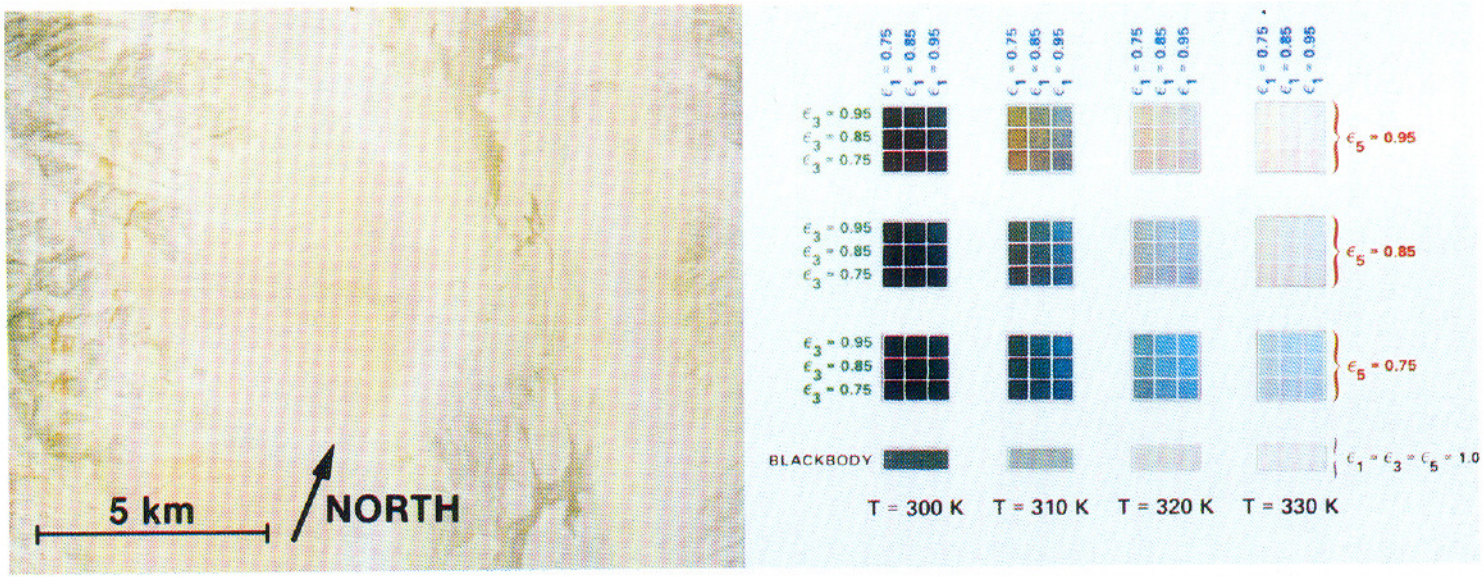

4a

FIGURE 4. NASA airborne TIMS daytime image of part of Death Valley, CA (22, July 1982), showing the effect of decorrelation stretching. The color pictures were constructed from three of six channels (ch. 1, 8.2–8.6 μm, B; ch. 3, 9.0–9.4 μm, G; ch. 5, 10.2–11.2 μm, R): (a) radiance data as acquired; (b) after linear stretch on each channel independently; (c) after severe linear stretch; (d) after decorrelation stretch. Color patches show data for representative temperatures T and emittances ε_i (color coded; subscript is channel number) processed along with the image data (Dicomed playback).


T = 300 K
T = 310 K
T = 320 K
T = 330 K
BLACKBODY
$\epsilon_5 = 0.95$
$\epsilon_5 = 0.85$
$\epsilon_5 = 0.75$
$\epsilon_1 = \epsilon_3 = \epsilon_5 = 1.0$
$\epsilon_3 = 0.95$
$\epsilon_3 = 0.85$
$\epsilon_3 = 0.75$
$\epsilon_1 = 0.95$
$\epsilon_1 = 0.85$
$\epsilon_1 = 0.75$

4b

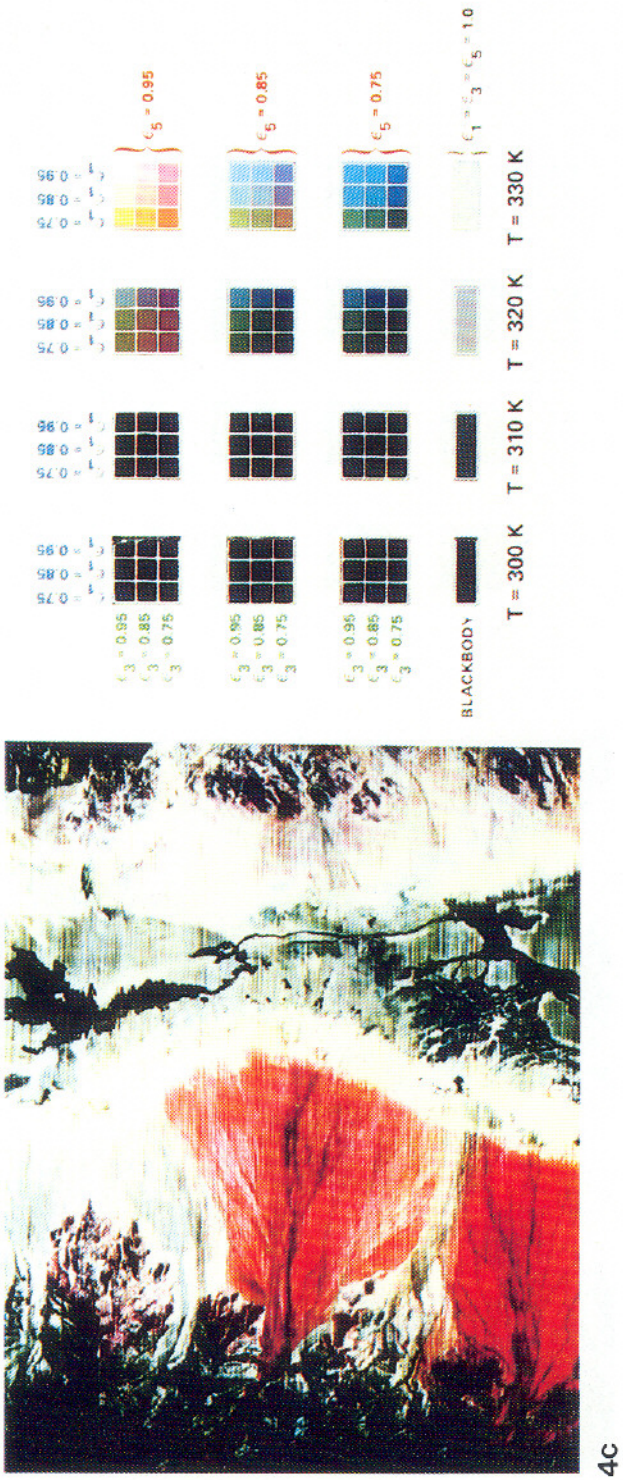
T = 300 K
T = 310 K
T = 320 K
T = 330 K
BLACKBODY
$\epsilon_5 = 0.95$
$\epsilon_5 = 0.85$
$\epsilon_5 = 0.75$
$\epsilon_1 = \epsilon_3 = \epsilon_5 = 1.0$
$\epsilon_3 = 0.95$
$\epsilon_3 = 0.85$
$\epsilon_3 = 0.75$
$\epsilon_1 = 0.95$
$\epsilon_1 = 0.85$
$\epsilon_1 = 0.75$

4C


T = 300 K
T = 310 K
T = 320 K
T = 330 K
BLACKBODY
$\epsilon_3 = 0.95$
$\epsilon_3 = 0.85$
$\epsilon_3 = 0.75$
$\epsilon_1 = 0.75$
$\epsilon_1 = 0.85$
$\epsilon_1 = 0.95$
$\epsilon_5 = 0.95$
$\epsilon_5 = 0.85$
$\epsilon_5 = 0.75$
$\epsilon_1 = \epsilon_3 = \epsilon_5 = 1.0$

4d

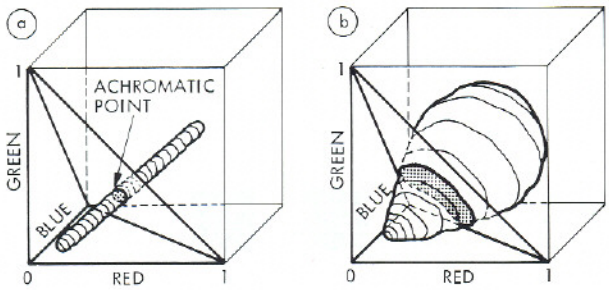

FIGURE 5. Schematic representation of decorrelation stretch of highly correlated data in three dimensions: (a) data as acquired fill the available volume poorly; (b) data after processing fill the volume optimally. The intersection of lines passing through the origin and the intensity triplets with the plane $R + G + B = 1$ defines the cluster in the $r'g'b'$ "chromaticity" diagram.

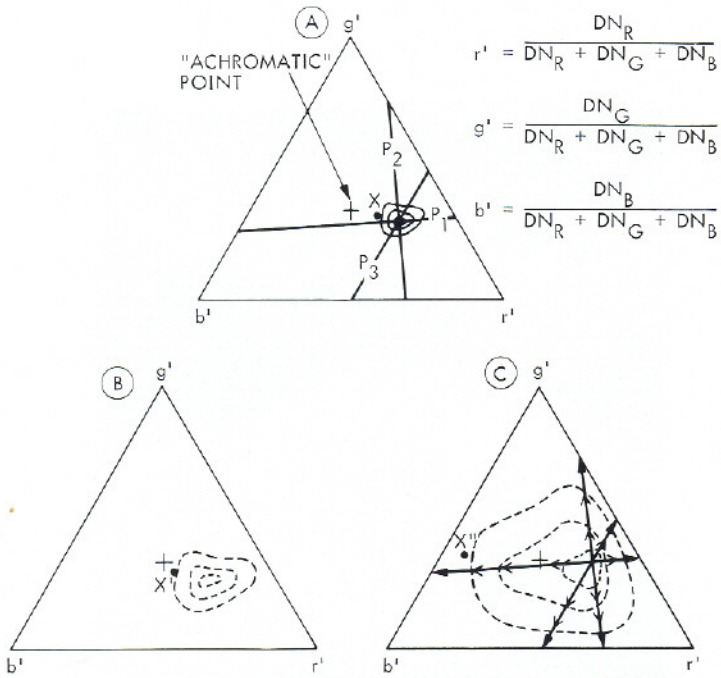

FIGURE 6. Image-domain "chromaticity" diagrams schematically showing the expansion of colors about the cluster center during linear and decorrelation stretches: (a) acquired data (projected principal axes are also shown); (b) linear stretch; (c) decorrelation stretch. The cluster was expanded along the projected principal axes. Point X in the acquired data cluster [Fig. 6(a)] is mapped to X' or X'' in the stretched clusters [Fig. 6(b) or (c)].

g', and b' (defined in Fig. 6) that describe "hue" and "saturation," but not intensity, of the DN triplets are displayed in the diagram.

Figure 6(a) shows a DN cluster for highly correlated images in which the principal axis P_1 does not coincide with the equal-intensity ("achromatic") axis ($R = G = B$). In the chromaticity diagram this cluster does not center on the "achromatic" point $r' = g' = b' = 0.333$. The projections of the three axes P_1, P_2, and P_3 are also shown in Fig. 6(a). As explained above, during conventional contrast stretching the cluster is expanded primarily along its principal axis P_1, or roughly normal to the plane of the chromaticity diagram. The effect is to enlarge the cluster of r', g', b' values only slightly [Fig. 6(b)], so that there is little increase of color in the displayed picture. Unstretched data plotting at X in Fig. 6(a) will be shifted only slightly to X' in Fig. 6(b).

During the decorrelation stretch the RGB data cluster is expanded along the other principal axes also [Fig. 6(c)]. Only if the centroid of the data cluster projects onto the "achromatic" point will "hue" in the image domain be invariant during the enhancement. Otherwise, the "hues" will be changed to some extent. In any case, perceived hues in the displayed data are not likely to be completely invariant, although practice has shown that deviations tend to be minor compared to the strong changes in the image domain described in this article.

An extreme example is shown in Fig. 6(c), where acquired data that plot at X in the unstretched cluster [Fig. 6(a)] are shifted outwards from the centroid through the "achromatic" point to X''. (As shown, image domain X corresponds to pastel orange in the display domain; X' is nearly gray; and X'' is saturated blue-green.) Resultant interpretive difficulties may be reduced by stretching the three images before decorrelation such that the mean values are brought into coincidence. In general, this will center the data cluster about the equal-intensity axis and the "achromatic" point. The decorrelation stretch will then produce colorful pictures in which the hues may be more easily interpreted, although they may not be faithful to the data as acquired. In practice, image data such as acquired by TIMS generally lie close to the equal-intensity axis and do not require prestretching.

Enhancement after HSI Transformation

In principal, contrast stretching following any of several data transformations may be equivalent to decorrelation stretching, at least in a general way. One transformation that has enjoyed popularity recently is the HSI or "hue"–"saturation"–intensity transformation (Gillespie, 1980). This coordinate system is attractive because the transformed parameters correspond approximately to the perceptual color attributes. It is emphasized that *HSI* coordinates describe the image domain; in the examples used in this article, the data are not even acquired in the visible part of the spectrum.

In the *HSI* transformation, the data in the assigned Cartesian coordinates (R, G, B) are recast in spherical coordinates (θ, ϕ, ρ), chosen such that the polar axis and the line $R = G = B$ coincide. H is equivalent to the longitude θ, and S and I are related to the colatitude (ϕ) and to the length of the DN vector (ρ), respectively.

Because the mathematics of the *HSI* transformation have been published with

minor errors by Gillespie (1980), the correct equations are summarized here [for a different, simpler "*IHS*" transformation see Buchanan (1979) and Haydn et al. (1982)]. The HSI transformation is depicted schematically in Fig. 7. Using the notation established above,

$$\theta = \tan^{-1}(-x/z) + n\pi,\ \phi = \cos^{-1}(y/r),$$
$$\rho = \sqrt{x^2 + y^2 + z^2},\ \phi \neq 0,$$
$$n = 2 \text{ if } z \leqslant 0,\ n = 1 \text{ if } z > 0,$$
$$x^2 + y^2 + x^2 \neq 0, \tag{1}$$

where (x, y, z) are Cartesian coordinates related to (R, G, B), as shown in Fig. 7. θ is a periodic function, and herein the color green is arbitrarily assigned to the branch cut. Thus 0 and 2π are "green," $2\pi/3$ is "red," and $4\pi/3$ is "blue." The polar axis of the spherical coordinate system (θ, ϕ, ρ) coincides with the main diagonal line ("achromatic" line or vector) of the RGB space. The two systems $(x, y, z \equiv R'', G'', B'')$ and (R, G, B) are related through two rotations that bring the line $R = G = B$ into coincidence with the y axis (the polar axis of the spherical space.) The rotations are 45° counterclockwise about the G axis and 54.7° counterclockwise about the new (rotated) R axis, if the coordinate systems are taken to be left-handed:

$$\begin{bmatrix} x \\ y \\ z \end{bmatrix} \equiv \begin{bmatrix} R'' \\ G'' \\ B'' \end{bmatrix} = \begin{bmatrix} 1 & 0 & 0 \\ 0 & \sqrt{1/3} & \sqrt{2/3} \\ 0 & -\sqrt{2/3} & \sqrt{1/3} \end{bmatrix} \times \begin{bmatrix} \sqrt{1/2} & 0 & -\sqrt{1/2} \\ 0 & 1 & 0 \\ \sqrt{1/2} & 0 & \sqrt{1/2} \end{bmatrix} \begin{bmatrix} R \\ G \\ B \end{bmatrix}. \tag{2}$$

Because the image data lie within the first quadrant of the *RGB* space, large values of ϕ do not occur: maximum values range from 35.3 to 54.7° as a function of $H \equiv \theta$. It is convenient to normalize ϕ by the maximum value $\phi_m(H)$ possible for a given value of H (details are given in Appendix B). Also a vector with a small colatitude ϕ can have a larger value of ρ than a vector with a large ϕ. This is important during enhancements in which ϕ is increased (as in this article), because it can lead to color shifts as one or more values of R, G, or B is forced overrange. Values of ρ are therefore normalized to the maximum value possible ρ_m for a given ϕ and H, or for a given R, G, B triplet (see Appendix C). Finally, "intensity" (I) is commonly regarded as the scalar sum of R, G, and B. To maintain this useful convention it is necessary to redefine (x, y, z) as $(\sqrt{R''}, \sqrt{G''}, \sqrt{B''})$ rather than (R'', G'', B'') as shown in Eq. (2):

$$\begin{bmatrix} x^2 \\ y^2 \\ z^2 \end{bmatrix} = \begin{bmatrix} \sqrt{1/2} & 0 & -\sqrt{1/2} \\ \sqrt{1/3} & \sqrt{1/3} & \sqrt{1/3} \\ \sqrt{1/6} & -\sqrt{2/3} & \sqrt{1/6} \end{bmatrix} \times \begin{bmatrix} R \\ G \\ B \end{bmatrix}. \tag{3}$$

The H, S, I space is thus defined by

$$H = \tan^{-1}(\sqrt{R''}/-\sqrt{B''}) + n\pi,$$
$$S = \cos^{-1}(\sqrt{G''}/\sqrt{B+G+R})\phi_m^{-1}(H),$$
$$I = (B+G+R)\rho_m^{-2}(B, G, R),$$
$$\phi \neq 0,\ n = 2 \text{ if } z \leqslant 0,\ n = 1 \text{ if } z > 0,$$
$$B + G + R > 0. \tag{4}$$

The goals of decorrelation stretching can

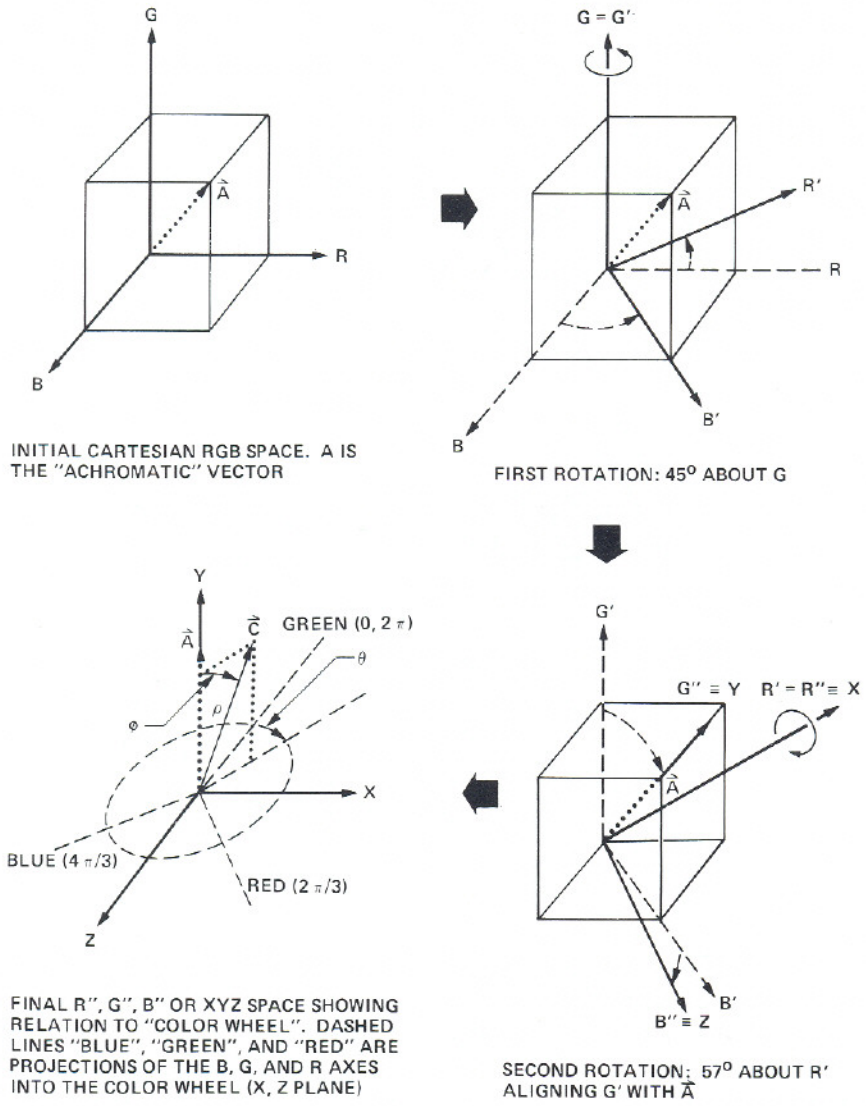

FIGURE 7. Coordinate transformation from RGB space to spherical coordinates $\theta\phi\rho$. Heavy arrows show the sequence of geometric operations described by Eq. (2). The final step in the figure shows the correspondence of spherical coordinates $\theta\phi\rho$ and Cartesian coordinates xyz [Eq. (1)], and also the orientation of the primary colors. HSI coordinates are related to $\theta\phi\rho$ by normalization (see text).

be achieved by stretching the S and I images before transformation back to the acquired data space for display. Figure 8(a) schematically illustrates the effect on the cluster from Fig. 6(a) of stretching S while leaving H unmodified. The probability density function (histogram) in Fig. 8(a) shows the histogram of the S image before and after contrast stretching. The effect on the cluster is to expand it along lines of constant H radiating from the "achromatic" point in the "chromaticity"

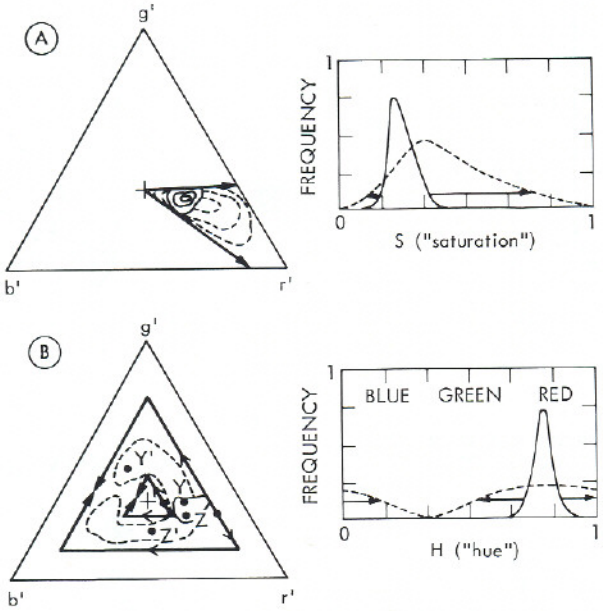

FIGURE 8. Color stretching in *HSI* coordinates affects data differently than decorrelation stretching, shown schematically by the image-domain "chromaticity" diagrams (left). Histograms (right) show "before" (solid contour lines) and "after" (dashed lines) data distributions in the transformed S and H images: (a) stretching S alone may result in a limited range of hues; (b) stretching H alone results in a cluster of limited "saturation" range in the "chromaticity" diagram. Colors that initially would have been very similar (Y, Z) may become very different (Y', Z').

diagram. The displayed picture would have a wide range of saturations, but a limited range of hues. It would appear almost monochromatic, with colors ranging only from orange to red.

Expansion of the range of hues in the displayed picture could be achieved by stretching the H image [Figure 8(b)]. This would smear the cluster along triangular trajectories of constant "saturation" in the $r'g'b'$ "chromaticity" diagram. Although the range of colors in the enhanced picture would be much greater, the picture might be difficult to interpret. Similar points Y and Z, both initially displayed as red-orange, could be transformed to Y' and Z', or green and magenta, respectively. As with the decorrelation stretch, stretching the acquired data before transformation to center the cluster over the "achromatic" point would reduce or remove this effect. In this case it would not be necessary to adjust the H image, because all possible values would already be present. However, the fidelity of the hues in the displayed picture compared to the acquired picture would be reduced.

The effects on the thermal image shown in Fig. 4 of stretching the S image alone and both the H and S images together are shown in Figs. 9(a) and (b), respectively. The inverse *HSI* transformation was applied after stretching and before

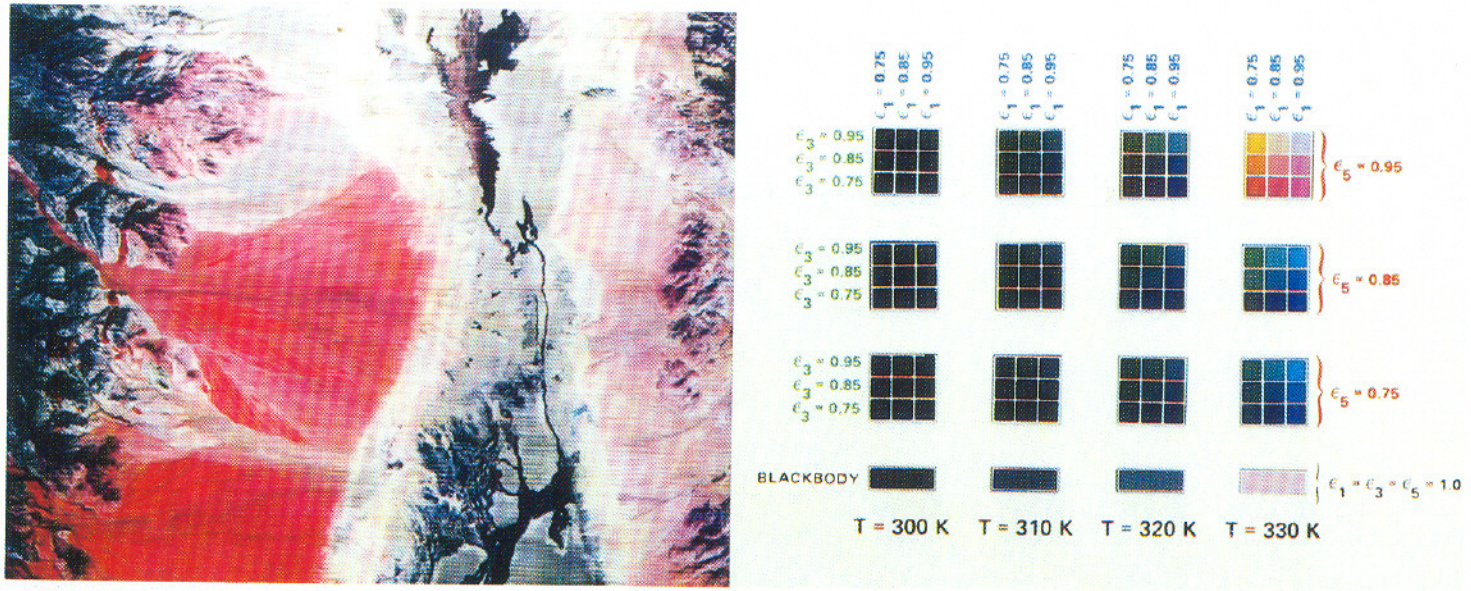

9a

FIGURE 9. Image of Fig. 4 enhanced by stretching transformed S and H channels. The intensity image was also stretched in each case: (a) effect of stretching S only; (b) effect of stretching both S and H. The H image was stretched to equalize the probability of encountering each possible value of H in the enhanced image. Data were transformed back from HSI to RGB coordinates for display. Color target is explained in Fig. 4.

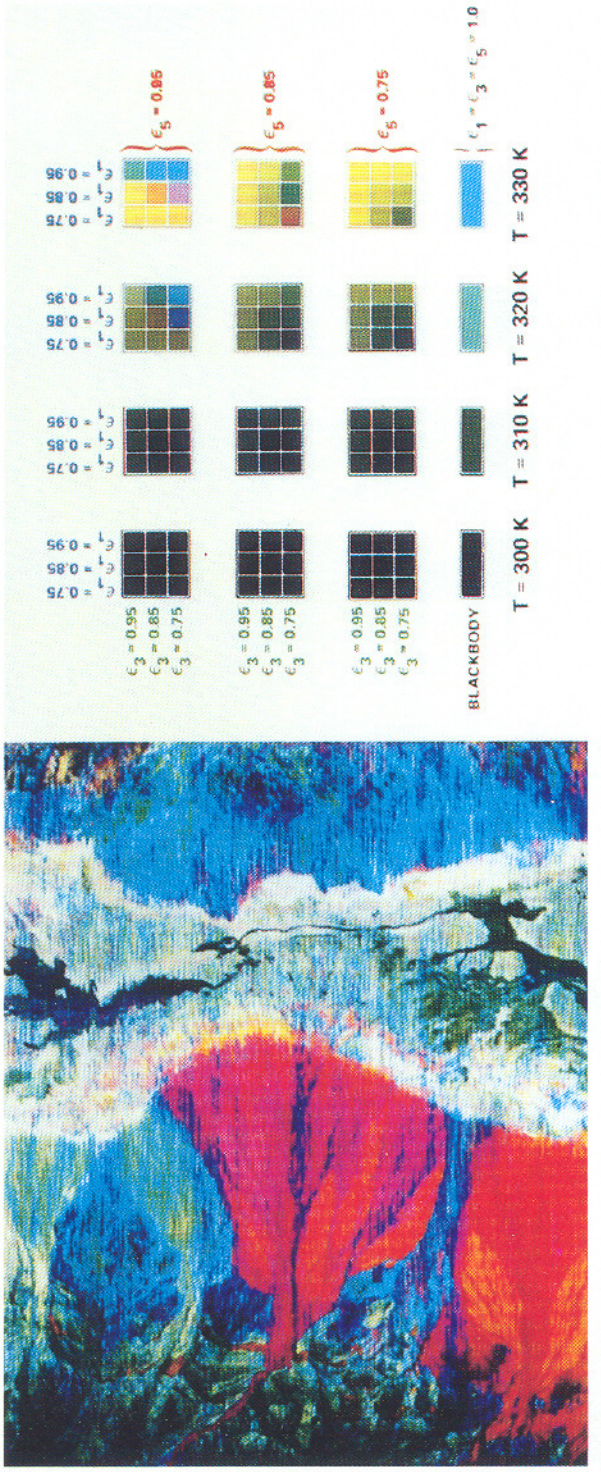
T = 300 K
T = 310 K
T = 320 K
T = 330 K
BLACKBODY
ϵ_3 = 0.95
ϵ_3 = 0.85
ϵ_3 = 0.75
ϵ_1 = 0.75
ϵ_1 = 0.85
ϵ_1 = 0.95
ϵ_5 = 0.85
ϵ_5 = 0.75
$\epsilon_1 = \epsilon_3 = \epsilon_5 = 1.0$

9b

construction of the color composite pictures.

Figure 9(a) resembles Fig. 6(b) (linear stretch) closely. Comparison of the color targets confirms this impression, although a greater range of temperatures are dark in Fig. 9(a). Figure 9(a) differs from Fig. 6(d) (decorrelation stretch) in that there are fewer greens and blues. This color shift probably is due to misalignment of the P_1 and equal-intensity axes, as discussed above.

The distribution of hues in Fig. 9(a) (H unmodified) is clearly different than in Fig. 9(b) (H stretched); perhaps this is best revealed by the detail in the red alluvial fans (lower center.)

Summary

It is difficult to effectively display color information from highly correlated images if conventional enhancement techniques are used. Instead, variables more closely related to perceptual color attributes—hue, saturation, and lightness—must be manipulated. There are a number of ways to do this, but we find that the most effective are based on transformation of the image data to new coordinates, enhancement of the transformed images, and retransformation to the original image coordinate system. The enhanced original images—not the transformed ones—are displayed as pictures. Retransformation is a vital step because it makes the color composite simpler to interpret.

The main goal of the enhancement procedure is to exaggerate color saturation while leaving hue substantially unchanged. Image intensity may or may not be stretched. We have reviewed two ways to achieve this. The first is based on a scene-dependent PC transformation that "decorrelated" the image data so that the deviations from gray or the average image color can be exaggerated. This technique is called the "decorrelation stretch." The second is based on the scene-independent HSI or "hue"–"saturation"–intensity transformation, in which the data are recast in spherical coordinates. In this approach the color saturation is adjusted directly, by stretching the S or "saturation" image.

One drawback of both the decorrelation and *HSI* techniques is that initially similar data may be displayed with greatly different, even complementary, hues if the acquired data do not center on the equal-intensity axis or "achromatic" point in the $r'g'b'$ "chromaticity" diagram. If the H ("hue") image is not stretched, the *HSI* method avoids this problem, but the range of hues in the color composite pictures may be severely limited. If the H image is stretched, the problem may be even more severe than for the decorrelation method.

Hue distortion may be eliminated or reduced in severity by equalizing the mean values of the acquired data before transformation, but this changes the average color and range of hues in the displayed picture. Experience has shown that these drawbacks are largely theoretical and that in practice the enhancements are both effective at displaying the spectral information contained in the acquired images and readily interpreted.

Appendix A.
Color Distortions During Playback

Chromaticities in color pictures made from digital images can be predicted from image-domain DN triplets if the characteristics of the playback device and the recording medium are known. In ideal

playback there would be a one-to-one correspondence between image intensities and picture transmittance or reflectance. Chromaticity coordinates in the display domain would have the same values as their counterparts in the image domain. This does not occur for many film recorders.

Below we illustrate chromatic distortions attending positive playback (creates positive transparencies) on JPL's GRE and Dicomed film recorders used to create the pictures of Figs. 3, 4, and 9. The playback was characterized using densitometer measurements of pictures of gray scales defined in the image domain. These measurements thus describe the combined playback and film characteristics. The Dicomed playback is exponential; the GRE playback is linear.

Exponential playback

The exponential Dicomed playback results in a linear relationship between photographic density D and image intensity DN:

$$D_i = D_{\max} - \frac{\mathrm{DN}_i}{\mathrm{DN}_{\max}}(D_{\max} - D_{\min}), \quad (0 \leqslant \mathrm{DN} \leqslant \mathrm{dn}_{\max}),$$
$$D_{\max} = 1.2,\ D_{\min} = 0.2, \qquad \text{(A1)}$$

where i denotes a primary color (R, G, B) in the picture or assigned to the corresponding image channel. $D_{\min}$ and $D_{\max}$ are the densities produced when $\mathrm{DN} = \mathrm{DN}_{\max}$ and $\mathrm{DN} = 0$, respectively. ($\mathrm{DN}_{\max} = 255$ for eight-bit recording of image intensities.) $D_{\max}$ and $D_{\min}$ are chosen such that the range of image intensities falls within the linear portion of the Hurter–Driffield (D–$\log E$) curve describing the response of the photographic medium to light.

Photographic densities are the logarithm of the transmittance τ, which is the fractional amount of light passed through the film (or reflected from a photographic print.) Thus $\tau = 10^{-D}$ and

$$\tau_i = 10^{-D_{\max}} 10^{-\mathrm{dn}_i(D_{\max} - D_{\min})}, \qquad \text{(A2)}$$

where $\mathrm{dn}_i \equiv \mathrm{DN}_i/\mathrm{DN}_{\max}$ is the fractional or normalized image intensity. Display-domain color may be described by chromaticity coordinates (r, g, b) calculated from the triplet of values of τ_i

$$r = \frac{\tau_R}{\tau_R + \tau_G + \tau_B},$$
$$g = \frac{\tau_G}{\tau_R + \tau_G + \tau_B}, \qquad \text{(A3)}$$
$$b = \frac{\tau_B}{\tau_R + \tau_G + \tau_B}.$$

Using Eqs. (A2), we can relate these chromaticity coordinates to dn_i, the normalized image-domain intensities:

$$r = \frac{10^{-\mathrm{dn}_R}}{10^{-\mathrm{dn}_R} + 10^{-\mathrm{dn}_G} + 10^{-\mathrm{dn}_B}},$$
$$g = \frac{10^{-\mathrm{dn}_G}}{10^{-\mathrm{dn}_R} + 10^{-\mathrm{dn}_G} + 10^{-\mathrm{dn}_B}}, \qquad \text{(A4)}$$
$$b = \frac{10^{-\mathrm{dn}_B}}{10^{-\mathrm{dn}_R} + 10^{-\mathrm{dn}_G} + 10^{-\mathrm{dn}_B}}.$$

Inspection of Eqs. (A4) shows that picture colors will generally tend to differ in both saturation and hue from the desired values specified in the image domain by analogous "chromaticity" coordinates:

$$r' = \frac{\mathrm{dn}_R}{\mathrm{dn}_R + \mathrm{dn}_G + \mathrm{dn}_B},$$
$$g' = \frac{\mathrm{dn}_G}{\mathrm{dn}_R + \mathrm{dn}_G + \mathrm{dn}_B}, \qquad \text{(A5)}$$
$$b' = \frac{\mathrm{dn}_B}{\mathrm{dn}_R + \mathrm{dn}_G + \mathrm{dn}_B}.$$

The chromatic shift during playback is a function of the image intensity, so that a single "chromaticity" (r', g', b') is mapped onto a trajectory of (r, g, b) values. Trajectories for Dicomed (exponential) playback for twelve values of (r', g', b') are shown on the left side of Fig. A-1.

Figure A-1 is an *rgb* chromaticity diagram that illustrates the color distortions caused by image playback. The diagram is organized to show the effects for three sets of the same four "hues," at different "saturations." For each "hue" specified in the image domain, there is a trajectory of possible *rgb* values that may be realized in the displayed picture (the trajectories also depend upon characteristics of the playback device.) The position on the trajectory is controlled by the image-domain "saturation" and intensity, $I \equiv \mathrm{DN}_R + \mathrm{DN}_G + \mathrm{DN}_B$. Thus, for any given

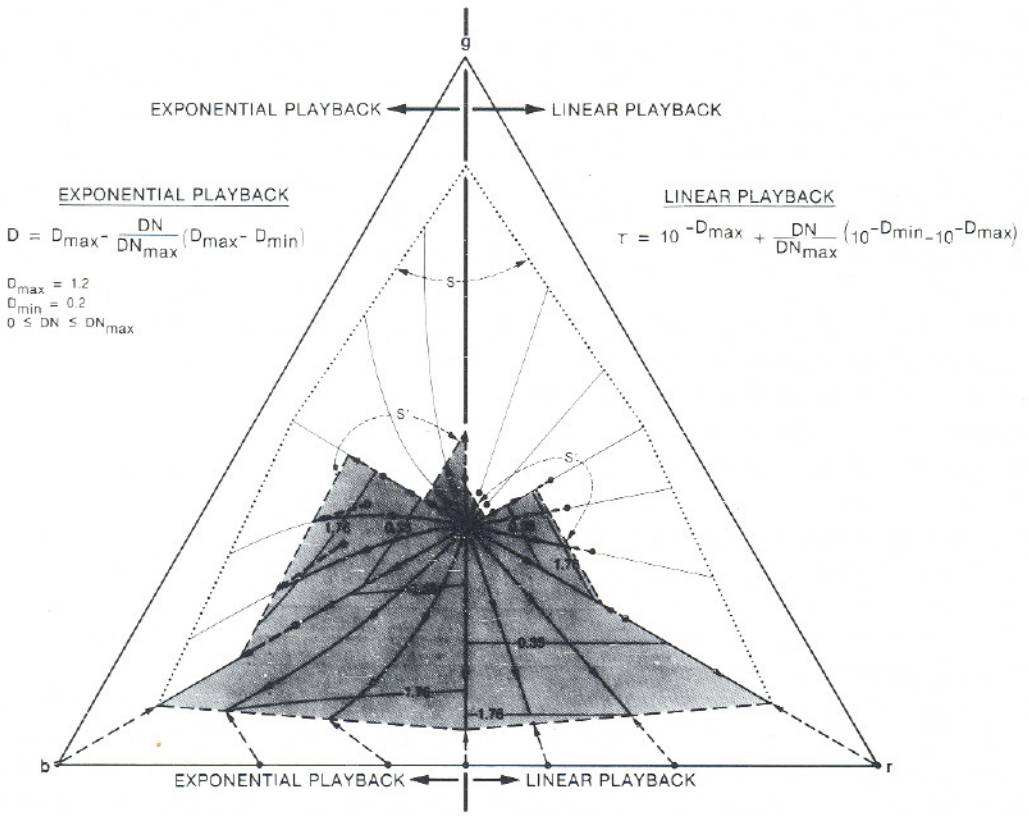

FIGURE A-1. An *rgb* chromaticity diagram showing chromatic distortions caused by recording digital images on color film. The left side shows effects of exponential playback; the right side illustrates linear playback. On each side, trajectories radiating from the diagram center show color changes as a function of image intensity, for 12 image "chromaticities." For ideal playback, display-domain and image-domain chromaticity coordinates would be the same: The image-domain chromaticities used in this illustration would plot on the heavy dots, not on the trajectories. The dots and their associated trajectories are connected by dashed lines. The pattern of chromaticity trajectories is repeated by reflection about the lines passing through the vertices and the center of the diagram. Thus there is a sixfold repetition of this pattern in the chromaticity diagram. This figure uses this redundancy to show three sets of image-domain chromaticities with the two playback modes. Each of the three sets of image-domain chromaticities contains the same four azimuths or "hues": a primary color, a secondary (complementary) color, and two intermediate hues at a single "saturation," or fractional distance from the center. See text for further explanation.

image-domain $r'g'b'$ triplet, Figure A-1 predicts the corresponding rgb values in the displayed picture, as a function of I.

In Fig. A-1, the chromaticity trajectories are shown by the lighter family of lines radiating from the diagram center, or the achromatic point ($r = g = b = 0.333$). The trajectories curve towards the vertices of the chromaticity diagram (saturated primary colors) as I is increased. At low intensities, τ_i is dominated by $D_{\max}$, which is the same for each of the three components of the color picture. Thus picture colors are unsaturated and their chromaticity coordinates plot near the achromatic point. As I is increased, τ_i is increasingly dominated by the term containing dn_i [Eq. (A2)] and the color becomes more saturated (hence the radiation of the trajectories from the achromatic point).

For a given image-domain "saturation," the part of the trajectory in Fig. A-1 that can actually be realized is shown by the heavier lines that follow the trajectories. The position along the trajectories as a function of image intensity is indicated by the lighter contour lines (the numbers 0.35 and 1.76 are intensity values normalized to $\mathrm{DN}_{\max}$).

For values of (r', g', b') plotting on or near the perimeter of the chromaticity diagram ("saturated" colors), one of the values DN_R, DN_G, or DN_B reaches its maximum limit $\mathrm{DN}_{\max}$ (or $\mathrm{dn}_i = 1$) before the trajectory of (r, g, b) value reaches an equivalent saturation. The locus of points at which this occurs for $D_{\max} = 255$ is shown by perimeter S in Fig. A-1. The distance of S from the diagram center depends upon the value of $\mathrm{DN}_{\max}$ and $D_{\max}$, but for finite values of these parameters no trajectory will reach the perimeter of the chromaticity diagram. Thus for highly "saturated" image-domain "colors," the corresponding colors in the picture will be undersaturated. Hues in light area in the picture will be shifted towards the nearest primary color, red, green, or blue, unless the image-domain "chromaticity" coordinates already correspond to a primary color or its complement.

For less "saturated" values of (r', g', b') that plot closer to the diagram center, the (r, g, b) coordinates follow the same trajectories, but at a different rate with respect to I. The perimeter S' at which DN_R, DN_G, or DN_B first attains a value of $\mathrm{DN}_{\max}$ is closer than S to the diagram center, but it is farther than (r', g', b'). Thus color saturation in the picture may be greater than desired for light areas of the picture. However, the hue distortion is not as great as it is for values of (r', g', b') plotting near the diagram perimeter.

Linear playback

For the GRE film recorder image playback was linear*:

$$\tau = 10^{-D_{\max}} + (10^{-D_{\min}} - 10^{-D_{\max}})\,\mathrm{dn}_i. \tag{A6}$$

Note that the image is still encoded in the linear part of the D–$\log E$ curve for the photographic film, independent of the playback device. Therefore, the picture has a finite transmittance (or reflectance) even if $\mathrm{DN} = 0$.

Chromaticity trajectories for the same 12 values of (r', g', b') used for illustrat-

*The GRE film recorder, constructed for playback of the Viking Lander images of the martian surface, was recently dismantled.

ing exponential playback are shown on the right side on Fig. A-1. For linear playback, hues are independent of image intensity I, and have the same value as the image-domain "hues" indicated by the coordinates (r', g', b').

However, saturations are a function of I, just as for exponential playback. In contrast to exponential playback, saturations never exceed the values specified in the image domain, but may approach them closely for high values of I. Thus even linear playback introduces chromatic distortions in color pictures.

Figure A-1 shows the chromaticity diagram in which the vertices represent the pure endmember colors, generally the dyes of the color film used to record the picture. Colors indicated in this diagram are relative to these primary colors. Their perceived values may be found if the actual chromaticity coordinates [e.g., in the CIE xyz system (Wyszecki and Stiles, 1967)] for the three end members and also for the illuminant are known. Geometrically, Fig. A-1 will project into a triangular subregion of the CIE chromaticity diagram, for which the vertices are the xyz coordinates of the film dyes [these xyz coordinates are not to be confused with the general Cartesian xyz coordinates of Eqs. (1)–(3)]. Only under specific circumstances will the center of the rgb chromaticity diagram—the equal-energy or "achromatic" point—coincide with the true achromatic point in the CIE xyz chromaticity diagram.

Appendix B. The Normalizing Function $\phi_m(H)$

The function $\phi_m(H)$ is periodic with three-fold symmetry in the interval 0 to 2π; that is, $\phi_m(H + 2n\pi/3) = \phi_m(H)$, for any integer n. $\phi_m(H)$ is the colatitude of an RGB vector that has the same "hue" H as the vector of interest, but that lies in one of the planes $B = 0$ $(0 \leqslant H < 2\pi/3)$, $G = 0$ $(2\pi/3 \leqslant H < 4\pi/3)$, or $R = 0$ $(4\pi/3 \leqslant H < 2\pi)$:

$$\phi_m(H) = \cos^{-1}\sqrt{1/3} \times \frac{-2B + G + R}{\sqrt{(B-G)^2 + (B-R)^2}} \qquad \left(0 \leqslant H < \tfrac{2}{3}\pi\right),$$

$$\phi_m(H) = \cos^{-1}\sqrt{1/3} \times \frac{B - 2G + R}{\sqrt{(G-B)^2 + (G-R)^2}} \qquad \left(\tfrac{2}{3}\pi \leqslant H < \tfrac{4}{3}\pi\right),$$

$$\phi_m(H) = \cos^{-1}\sqrt{1/3} \times \frac{B + G - 2R}{\sqrt{(R-B)^2 + (R-G)^2}} \qquad \left(\tfrac{4}{3}\pi \leqslant H < 2\pi\right).$$

Appendix C. The Normalizing Function ρ_m

The function ρ_m is the length of an RGB vector that has the same "hue" H and colatitude ϕ as the vector of interest, but that ends in one of the planes $R = W$ $(\pi/3 \leqslant H < \pi)$, $G = W$ $(-\pi/3 \leqslant H < \pi/3)$, or $B = W$ $(\pi \leqslant H < 5\pi/3)$, where W is the largest value possible for R, G, or B (e.g., because of encoding as a finite number of bits; for eight-bit data, $W = 255$):

$$\rho_m = \rho W/R \qquad (\pi/3 \leqslant H < \pi),$$

$$\rho_m = \rho W/G \qquad (-\pi/3 \leqslant H < \pi/3),$$

$$\rho_m = \rho W/B \qquad \left(\pi \leqslant H < \tfrac{5}{3}\pi\right).$$

John Reimer prepared the color targets for Figs. 3 and 7. Michael Abrams processed the Landsat image. We appreciate the contributions to the logic and lore of decorrelation stretching by IPLers past and present: James Soha, Arnold Schwartz, Daryl Madura, John Reimer, and Ronald Alley. Discussions with Michael Abrams, Harold Lang, Frank Palluconi, and Melvin Podwysocki, and criticisms by Melvin Podwysocki and two anonymous reviewers improved the manuscript. This research was performed at the Jet Propulsion Laboratory of the California Institute of Technology under contract to the National Aeronautics and Space Administration.

References

Abrams, M. (1984), Landsat-4 Thematic Mapper simulator data for a porphyry copper deposit, *Photogramm. Eng. Remote Sens.* 50:1171–1173.

Berlin, G., Chavez, P., Grow, T., and Soderblom, L. (1976), Preliminary geologic analysis of Southwest Jordan from computer enhanced Landsat-1 image data, *Proc. American Society of Photogrammetry*, 42nd Annual Meeting, 22–28 February.

Buchanan, M. D. (1979), Effective utilization of color in multidimensional data presentation, *Proc. Soc. Photo-Opt. Eng.* 199:9–19.

Catmull, E. (1979), A tutorial on compensation tables, *Comput. Graphics* 13:1–7.

Daily, M. (1983), Hue–saturation–intensity split-spectrum processing of Seasat radar imagery, *Photogramm. Eng. Remote Sens.* 49:349–355.

Foley, J. D., and Van Dam, A. (1982), *Fundamentals of Interactive Computer Graphics*, Addison-Wesley, Reading, MA, 664 pp.

Gillespie, A. R. (1975), Color manipulation of digital images, *Proc. Society of Photographic Scientists and Engineers Symposium IV, Unconventional Photographic Systems*, 20–21, November, Washington, DC, pp. 35–37.

Gillespie, A. R. (1980), Digital techniques of image enhancement, in *Remote Sensing in Geology*, (B. S. Siegal and A. R. Gillespie, Eds.) Wiley, New York, 702 pp.

Gillespie, A. R., Kahle, A. B., and Palluconi, F. D. (1984), Mapping alluvial fans in Death Valley, California, using multispectral thermal infrared images, *Geophys. Res. Lett.* 11:1153–1156.

Gillespie, A. R., Kahle, A. B., and Walker, R. E. (1986), Color enhancement of highly correlated images: II. Channel ratio and chromaticity transformation techniques, *Remote Sens. Environ.*, forthcoming.

Gonzalez, R. C., and Wintz, P. (1977), *Digital Image Processing*, Addison-Wesley, Reading, MA, pp. 103–112 and 309–317.

Haydn, R. (1981), The application of a colour transformation for the enhancement of multispectral images and for the combination of multisensor data, *Summaries: International Symposium on Remote Sensing of the Environment, "Remote Sensing of Arid and Semi-Arid Lands,"* 3–9 November Cairo, Egypt, p. 78.

Haydn, R., and Youssef, M. (1984), The application of processed Landsat imagery in photo-interpretation, *Proc. International Geoscience and Remote Sensing Symposium, Vol. I*, June, Munich, Germany, p. TP-9.5.

Haydn, R., Dalke, G. W., Henkel, J., and Bare, J. E. (1982), Application of the IHS color transform to the processing of multisensor data and image enhancement, *Proc. International Symposium of Remote Sensing of the Environment, "Remote Sensing of Arid and Semi-Arid Lands,"* Cairo, Egypt, January, pp. 599–616.

Hotelling, H. (1933), Analysis of a complex of statistical variables into principal compo-

nents, *J. Educ. Psychol.* 24:417–441, 498–520.

Kahle, A. B., and Rowan, L. C. (1980), Evaluation of multispectral middle infrared images for lithologic mapping in the East Tintic Mountains, Utah, *Geology* 8:234–239.

Kahle, A. B., and Goetz, A. F. H. (1983), Mineralogic information from a new airborne thermal infrared multispectral scanner, *Science* 222:24–27.

Kahle, A. B., and Walker, R. E. (1984), Calculation of emissivity and thermal inertia at Death Valley, California, from TIMS data, *Proc. 9th Canadian Symposium on Remote Sensing*, August, St. John's, Newfoundland, Canada, pp. 337–345.

Kahle, A. B., Madura, D. P., and Soha, J. M. (1980), Middle infrared multispectral aircraft scanner data: analysis for geologic applications, *Appl. Opt.* 19:2279–2290.

Kruse, F. A., and Raines, G. L. (1984), A technique for enhancing digital color images by contrast stretching in Munsell Color Space, *Proc. International Symposium on Remote Sensing of Environment, 3rd Thematic Conference*, Environmental Research Institute of Michigan, Colorado Springs, CO, p. 121.

Meyer, G. W., and Greenberg, D. P. (1980), Perceptual color spaces for computer graphics, *Comput. Graphics* 14:254–261.

Palluconi, F. D., and Meeks, G. R. (1985), Thermal Infrared Multispectral Scanner (TIMS): An investigators' guide to TIMS data, JPL Publication 85-32, Jet Propulsion Laboratory, Pasadena, CA, 22 pp.

Pearson, K. (1901), On lines and planes of closest fit to a system of points in space, *Phil. Mag.* 2, *6th Ser.*:557–572.

Raines, G. L. (1977), Digital color analysis of color-ratio-composite Landsat scenes, *Proc. 11th International Symposium on Remote Sensing of the Environment*, pp. 1463–1472.

Ruiz, R. M., Elliott, D. A., Yagi, G. M., Pomphrey, R. B., Power, M. A., Farrell, K. W., Jr., Lorre, J. J., Benton, W. D., Dewar, R. E., and Cullen, L. E. (1977), IPL processing of the Viking Orbiter images of Mars, *J. Geophys. Res.* 82:4189–4202.

Smith, A. R. (1978), Color gamut transformation pairs, *Comput. Graphics* 12:12–19.

Soha, J. M., and Schwartz, A. A. (1978), Multispectral histogram normalization contrast enhancement, *Proc. 5th Canadian Symposium on Remote Sensing*, Victoria, BC, Canada, pp. 86–93.

Soha, J. M., Gillespie, A. R., Abrams, M. J., and Madura, D. P. (1976), Computer techniques for geological applications, *Proc. Caltech/JPL Conference on Image Processing Technology*, Data Sources and Software for Commercial and Scientific Applications, California Institute of Technology, Pasadena, CA.

Taylor, M. M. (1973), Principal components color display of ERTS imagery, *Third Earth Resources Technology Satellite-1 Symposium*, 10–14, December, NASA SP-351, Vol. 1, Section B, pp. 1877–1897.

Thomas, I. L., and Nicholas, J. V. (1984) Special colour enhancement for three channels having similar radiances, *Int. J. Remote Sens.* 5:753–760.

Williams, R. S., Jr. (1983), Geological applications, in Manual of Remote Sensing, II (R. N. Calwell, J. E. Estes, and G. A. Thorley, Eds.) 2nd ed., American Society of Photogrammetry, Falls Church, VA, pp. 1667–1953.

Wyszecki, G., and Stiles, W. S. (1967), *Color Science*, Wiley. New York, 628 pp.

Received 30 September 1985; revised 28 March 1986.

Erratum: Gillespie, A. R., Kahle, A. B., and Walker, R. E. (1986), Color enhancement of highly correlated images. I. Decorrelation and HSI Contrast Stretches, *Remote Sens. Environ.* 20: 209–235.

On page 217, left column, line 16, the figure number should be Fig. 4(b) rather than Fig. 4(d) as shown.

On page 229, left column, line 3, the figure number should be Fig. 4(b) rather than 6(b) as shown.

Figure A-1, which appears on page 231, is reproduced correctly below.